Journal of Engineering and Sustainable Development
http://jeasd.uomustansiriyah.edu.iq/index.php
https://doi.org/10.31272/jeasd.25.5.8

Vol. 25, No. 05, September 2021
ISSN 2520-0917

PERFORMANCE ASSESS OF SELF-EXCITED IG DRIVEN BY WIND TURBINE WORKING WITH FC-TCR

***Mohammed M. Khalaf[1]** **Amer M. Ali[1]**

1) Electrical Engineering Department, College of Engineering, Mustansiriyah University, Baghdad, Iraq

Received 22/2/2021 ***Accepted in revised form 1/5/2021*** ***Published 1/9/2021***

Abstract: This work presented a self-excited induction generator (SEIG) model controlled by an (FC-TCR) fixed capacitor-thyristor control reactor consisting of a large fixed capacitor in parallel with a thyristor controlled reactor in series with the constant inductance. Induction machines were used because they are capable of working at different speeds. The 3-phase IG was driven by the prime mover that represents the wind turbine. Also, constant voltage and frequency were obtained, regardless of the change in velocity, by using proportional integration (PI control) for each of them. This type of generator is used in isolated rural areas far from power transmission lines. The voltage and frequency are analyzed for each wind speed proposed in the model and calculating the required excitation amplitude and torque required to drive the induction generator. Therefore, it is now a key interest to develop an efficient, viable, economic, and controllable induction generator for harnessing energy from renewable sources. The strategy of control was implemented with MATLAB/Simulink.

Keywords: *SEIG, FC-TCR, Wind Turbine, MATLAB/Simulink.*

1. Introduction

Meeting the energy demand of the rising population from traditional energy sources, such as coal, gas, etc., has become very difficult. Power companies have now turned their focus to non-conventional energy sources such as wind, solar, biogas, etc., to address these problems, as they are available in abundance, sustainable, and environmentally friendly. The main objective is the production of economical and effective power generators [1]. Due to their simplicity and advantages, squirrel cage induction generators equip a significant part of the wind turbine generator in mini power plants. Once the machine shaft is driven to rotate above synchronous speed, regeneration operation is automatic [2]. There is no external reactive power in the stand-alone operating mode, and the generator must be self-excited. This problem can be solved by connecting the suitable capacitor bank with stator terminals in the system. This operating mode is highly valued since, and thus decentralized electrical sources are allowed to do so. HOWEVER, the SEIG dynamical behavior becomes more complicated because of the wind speed, the exciting capacitance, and the variance in load demand will significantly affect voltage and frequency [3]. Jyotirmayee proposed a bidirectional PWMSI connected to the IG and operated in closed-loop control mode with a DC-link battery to maintain the voltage and frequency [4]. Khaled investigates the impact of converting AC–DC power on the generator, the self-excited IG's dynamic performance during start-up [5]. Ramachandran presents a procedure

**Corresponding Author*: mhmdhss42229@gmail.com

based on a (GA) for the performance predetermination of wind-driven SEIGs operating in parallel [6]. Toufik proposes the extreme-seeking control algorithm method by using (MPPT) as a control solution to drive the average position of the operating point near to optimality [7]. Yu Wang presented method (ITIBC), which are a group of optimal switch vectors used to achieve the shortest recovery time and the minimum number of output voltage changes without overshooting [8] Yupeng proposed a power electronic converter based SEIG emulator developed using the dSPACE to investigate the SEIG operation under unbalanced conditions [9]. The research aims to use an FC-TCR control system to regulate both voltage and frequency under different loads and variable wind speeds. The paper examines and contributes to the voltage build-up behavior of SEIG and frequency under different loading conditions in a clear and distinct manner via the proposed control system. The Matlab/ Simulink program is adopted for this work.

1.1 System of SEIG

"Fig. 1", Shows the global SEIG system configuration proposed for operating in remote and isolated locations far from power transmission lines. This asynchronous generator IG, which operates in independent mode, can provide electrical power to the resistive load and inductive load, considering the wind as a prime mover. In this configuration, the capacitor bank provides the reactive power (VAR) needed for generator magnetization and the load. This chapter begins by discussing SEIG and its modeling. [10]

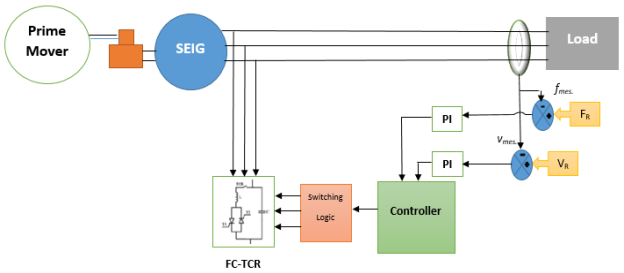

Figure 1. Block diagram for a SEIG controlled by a branch of FC-TCR

2. FC-TCR Operation

The system of SEIG is controlled by an FC-TCR consisting of a large fixed capacitor in parallel with a fixed inductance in series with a thyristor-controlled reactor. According to the branch (TCR), output voltage and frequency are regulated by compensating either increase or disease of the reactive power system depending on the load conditions and the prime mover. [11] The system included a wind power-driven three-phase induction generator, which operates in a stand-alone system and supplies a resistive and inductive load. The reactive power supply is supplied from the FC-TCR circuit to maintain a constant output voltage and constant frequency. From a frequency and voltage PI controller, the firing angle α is obtained to turn on or off the anti-parallel thyristors. System voltage and frequency are compared to the reference voltage and reference frequency. The error signal (feedback) is applied to a control system that provides the required firing angles α to the 3-phase static VAR compensator [12]. The suggested scheme is FC-TCR type. This assures a variable leading current by varying the drop voltage on the reactor; this equivalents a variable capacitor bank "Fig. 2", Shows a per phase simplified diagram of an FC-TCR.

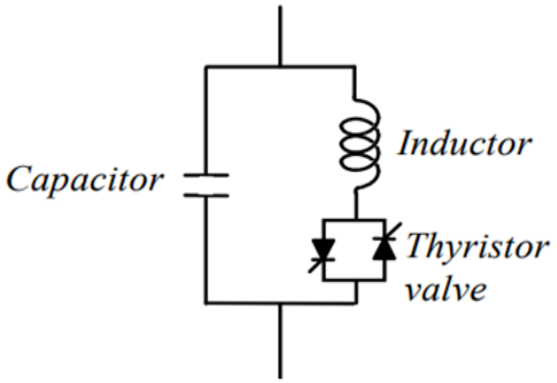

Figure 2. An FC-TCR Branch per Phase

Each phase consists of one reactor, controlled by a back-to-back thyristor switch, supplied by one or more fixed capacitor banks. The reactance impedance is rated to equal the maximum required value of capacitance impedance. The largely required reactor in FC-TCR can be a source of odd harmonics, which its magnitude has a proportional relationship with the size of FC-TCR. The amount of supplied reactive power is controlled by controlling the current through the reactor by controlling the period's duration in each half cycle by issuing gating pulses to the thyristors. The thyristor is self-commutates at every current zero. Therefore the current through the reactor is achieved by firing the thyristor at the desired firing angle α concerning waveform of the voltage.

3. Process of The Self-Excitation

The direction of induced torque is reversed when an IM is powered by an external prime mover that runs faster than the synchronous speed (negative slip) and begins working as an induction generator. The real power flows out of the system, but the machine requires reactive power. In the conversion of wind energy systems applications, the key disadvantage of the induction generator is the need for leading reactive power to build up terminal voltage and produce electric power. This leading reactive power can be generated by the use of a terminal capacitor across generator terminals.

A small terminal voltage is generated by residual magnetism present in the rotor iron 0-Er1 across stator terminals when the rotor of the induction machine is operated at the required speed. This voltage creates a capacitor current o-a. This current generates a flux that supports the residual flux, thus generating more flux and producing more voltage across b-Er2-represented stator terminals. In the capacitor bank, this voltage sends a current that ultimately produces the d-Er2 voltage. This cumulative voltage build-up process continues until the induction generator saturation curve intersects the capacitor load line at a point called the operating point. As shown in "Fig. 3", the voltage build-up affects the capacitor value. The higher the capacitance value, the greater the voltage build-up.

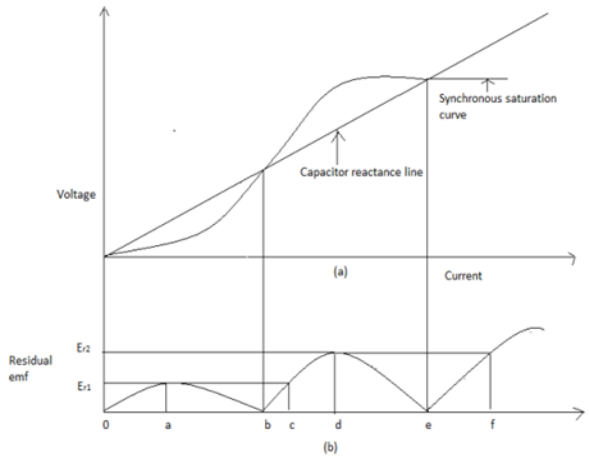

Figure 3. Voltage Build-up in a Self-Excited IG (a) The Capacitor Load Line & the Saturation curve, (b) Difference Between Them [13].

4. Mathematical Background

4.1 Wind Turbine [14-15]

The simple wind turbine theory through which we can apply Newton's laws in mechanics, where it is assumed here that the airflow (axial and centered towards the wind turbine) shows that the

energy acquired by the turbine is part of the energy possessed by the wind. The kinetic energy in the varying wind turbine speed is converted into mechanical energy by the wind turbine rotor, the kinetic energy of air currents that have mass (***m***) and move at speed (***v***) is given by the relation:

$$E = \frac{1}{2} m v^2 \quad (1)$$

Since wind turbine have blades and each has a certain length (R), the area of the circle (A) is equal to:

$$A = \pi R^2 \quad (2)$$

Then the wind will form a tube that has an area of (***A***), which follows that the mass is given in the following relationship:

$$m = \rho A v \quad (3)$$

m, the mass of air. **ρ**, the density of air. ***A***, turbine swept area. ***v***, wind speed.

By substituting Equation 3 in Equation 1, the kinetic energy of the wind is produced. It becomes clear to us that the energy affecting the wind turbine depends on the area ***A*** that the blades make as they rotate and on the density **ρ** and velocity ***v*** of the air, and the latter is the most influential factor due to the third force:

$$E = \frac{1}{2} \rho A v^3 \quad (4)$$

The coefficient that goes into determining the production efficiency of the wind turbine in the production of electrical energy and this efficiency is usually determined by the energy that the turbine acquires from the energy provided by the wind, and thus the power coefficient C_p of the rotor and can be defined as the ratio between the wind mechanical output power P_w of the rotor to the power possessed by the wind E, which is given by the relation:

$$C_p = \frac{2P_w}{\rho A v^3} \quad (5)$$

Then the wind mechanical output power is:

$$P_w = \frac{1}{2} \rho C_p A v^3 \quad (6)$$

The ratio between the tip-speed of the rotor **λ** and the wind speed ***v*** is expressed in the following relationship:

$$\lambda = \frac{R\ \omega}{v} \quad (7)$$

$$\omega = \frac{2\pi N}{60} \quad (8)$$

λ, is the tip-speed ratio. ω, the angular velocity ***N***, the rotational speed.

4.2 SEIG

The d-q axis model of an induction machine has been commonly used; under three-phase balanced conditions, the model is typically modified to analyze the machine's performance. The findings obtained from the d-q axis induction machine model can become very complicated if the device is studied under an unbalanced three-phase operating condition, as a zero induction machine model will be very difficult, the zero axis quantity will be produced leads to the zero sequence component [16].

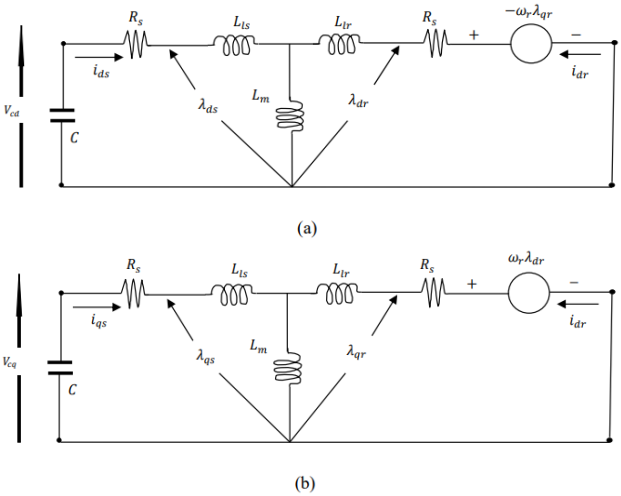

Figure 4. D-Q axes of an IG, (a) D-axis, (b) Q-axis

Rearranging the terms after taking the loop for "Fig. 4", we can writing equations:

$$V_{ds} = r_s.i_{ds} + P\lambda_{ds} \quad (9)$$
$$V_{qs} = r_s.i_{qs} + P\lambda_{qs} \quad (10)$$
$$V_{dr} = r_r.i_{dr} + P\lambda_{dr} + \omega.\lambda_{qr} \quad (11)$$
$$V_{qr} = r_r \cdot i_{qr} + P\lambda_{qr} - \omega \cdot \lambda_{dr} \quad (12)$$

V_{ds},V_{qs}, i_{ds}, and i_{qs} Are the stator voltages and currents. V_{dr},V_{qr}, i_{dr}, and i_{qr} Are the rotor voltages and currents. λ_{ds}, λ_{qs}, λ_{dr} and λ_{qr} Are the stator and rotor fluxes, respectively. r_s and L_{ls} Are the resistance and the self-inductance of the stator. r_r and L_{lr} Are the resistance and the self-inductance of the rotor.

The electromagnetic torque can be expressed in terms of the stationary reference variables by [17-18]:

$$T_{em} = \frac{3}{2}\frac{P}{2}(\lambda_{ds}.i_{qs} - \lambda_{qs}.i_{ds}) \quad (13)$$

4.3 Estimation of Excitation Capacitance

The value of the excitation capacitance (maximum and minimum) can be calculated as follows [19]:

$$S^2 = P^2 + Q^2 \quad (14)$$
$$S = \sqrt{3} \times V_{\text{line}} \times I_{\text{line}} \quad (15)$$
$$P = S\cos\theta \quad (16)$$
$$Q = \sqrt{(S^2 - P^2)} \quad (17)$$
$$Q_{\text{phase}} = \frac{Q}{3} \quad (18)$$
$$C_{max.} = \frac{Q}{2\pi f(V_{line})^2} \quad (19)$$
$$C_{min.} = \frac{1}{2\pi f X_m} \quad (20)$$

5. System Modelling by Matlab/Simulink

Table. 1 and Table. 2 show the all information about the machine that use in this work with the turbine:

Table 1. SEIG-Parameters

Parameters	Values	Units
Rated Power	15	kW
Rated Voltage	400	V
Rated Current	29	A
Frequency	50	Hz
Poles Number	4	pole
Resistance of stator	0.2147	**Ω**
Resistance of rotor	0.2205	**Ω**
Inductance of stator	0.000991	H
Inductance of rotor	0.000991	H

Table 2. Wind Turbine Parameters

Parameters	Values	Units
Blade Radius	5.5	m
Pitch Angle	0°	Deg.
Gear Ratio	90	-
Rated Wind Speed	4-14	m/s

The different wind speeds were represented using a ready-made block in the program called the signal builder and taking different values that simulate the wind speed (4, 8, 6, 12, 10, and 14 m/s) as shown in "Fig. 5"

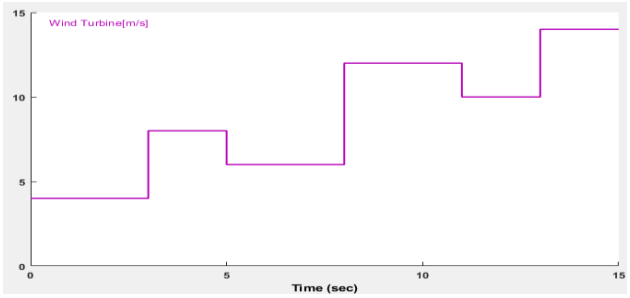

Figure 5. Wind Speed Representation in Matlab/ Simulink

The wind speed was converted from m / s (meter per second) to r.p.m (revolution per minute) to simulate the mechanical input of a self-excited induction generator by using the equation which converts the velocity from linear velocity (which was simulated as a different wind speed) to

rotational velocity (which represents the mechanical speed for entering the SEIG) and using a fixed gear ratio mechanical of the turbine approved in previous references.

In this system, the building behavior of the voltage, current, and frequency was studied at a period and within (15sec.), and the programmatic results proved the construction state and the stability of the self-excited inductive generator work for each load condition and the total time were divided into certain periods each period simulating a certain wind speed, for example, the period from (0 - 3 sec.) corresponds to a wind speed of 4 m/s, and from (3 - 5sec.) corresponds to 8 m/s, and from (5 - 8sec.) corresponds to 6 m/s, and from (8 - 11sec.) it corresponds to 12 m/s. From (11-13sec.), it corresponds to 10 m/s, and finally, the period from (13-15 sec.) corresponds to wind speed of 14 m/s. "Fig. 6", shows the complete SEIG model.

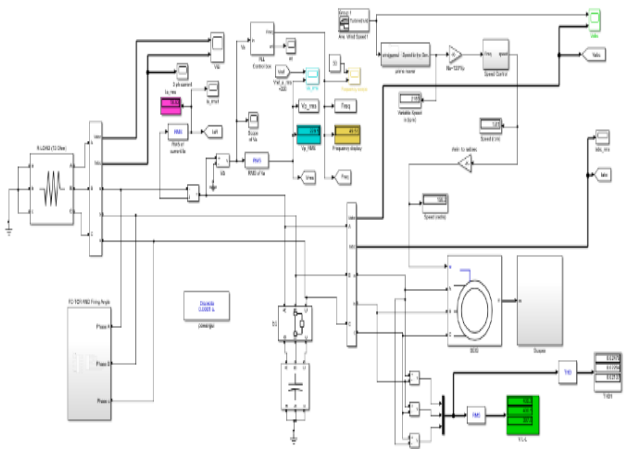

Figure 6. Complete SEIG model

1. Results and discussion

Case (1) at unity power factor for R-load (13Ω) with variable speed wind turbine, we listed the results in table 3. The values of each of the voltage, frequency and current and compare them with the case of inductive load, which we will deal with later.

Table 3. Case (1) SEIG results under resistive load

Wind speed [m/s]	Prime Mover Speed [r.p.m]	F [Hz]	$V_{ph.}$ [V]	$I_{ph.}$ [A]
4	625	49.3	238.9	19.38
8	1250	49.34	238.5	19.26
6	937.6	49.32	238.9	19.28
12	1875	49.35	239.8	19.28
10	1563	49.32	240.1	19.49
14	2188	49.33	242.1	19.46

The three-phase sine wave signal at any variable speed under resistive load was shown in "Fig. 7",

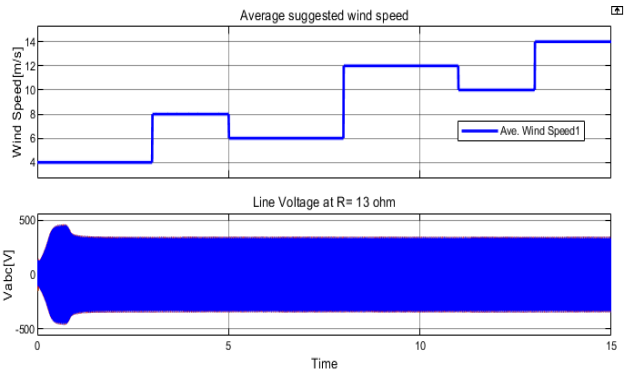

Figure 7. Line Voltage under R-Load with variable speed

The THD is an index of the closeness in shape between the waveform and its fundamental component and is defined as [20]

$$THD = [\left(\frac{v}{v_1}\right)^2 - 1]^{1/2} \quad (21)$$

Where, V_1 is the voltage fundamental R.M.S component.

The (THD) shown in "Fig. 8", At start time 5s with 6 m/s is 2.84%, and in 11s with 10m/s is 2.48%.

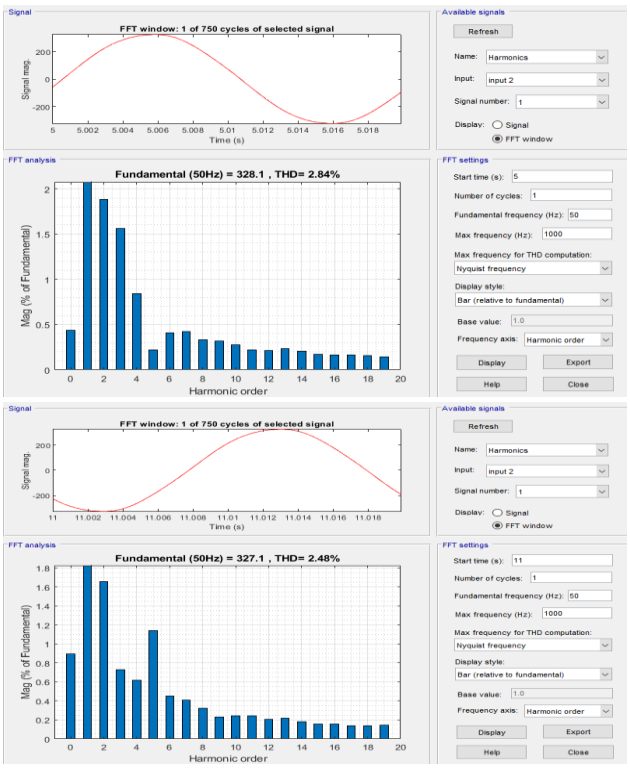

Figure 8. Total Harmonic Distortion in R- Load

"Fig. 9", shows the electromagnetic torque generated by SEIG.

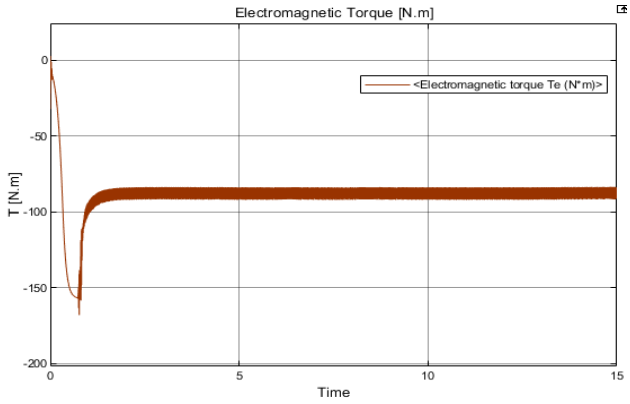

Figure 9. Electromagnetic Torque Generated

The three-phase currents with resistive load were shown in "Fig. 10".

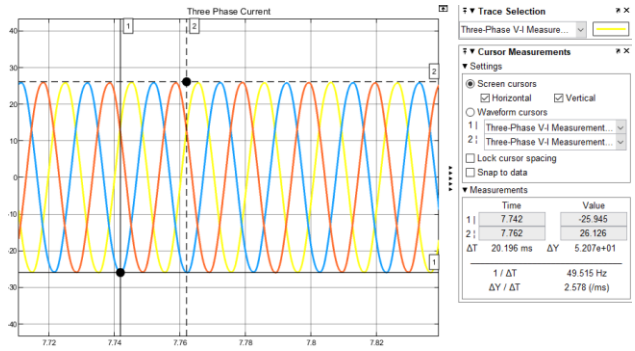

Figure 10. Three- Phase currents under R-Load

Case (2) at a (0.85) lagging power factor with RL-load (R=12$\boldsymbol{\Omega}$ and L=0.6$\boldsymbol{m}$H) with variable speed wind turbine. The results of this case were shown in table. 4 the values of each of the voltage, frequency and current, as more current was consumed in this case and the frequency is less when compared with the case of the load resistance only. And "Fig. 11" It shows the three-phase voltage wave and the current stability of the system and reading the frequency values.

Table 4. Case (2) SEIG results under RL-Load

Wind speed [m/s]	Prime Mover Speed [r.p.m]	F [Hz]	$V_{ph.}$ [V]	$I_{ph.}$ [A]
4	625	49.25	226.8	19.87
8	1250	49.25	230	20.04
6	937.6	49.25	232.1	20.23
12	1875	49.28	229.6	20.04
10	1536	49.27	230.6	20..3
14	2188	49.26	230.7	20.02

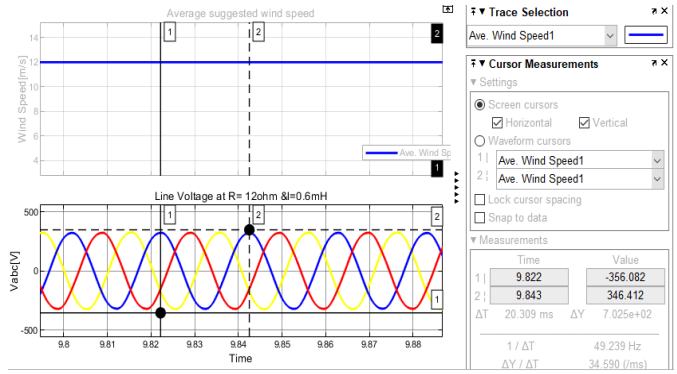

Figure 11. Three phase voltage & Frequency

The three-phase voltage signal is stable at any wind speed under the inductive load, as shown in "Fig. 12".

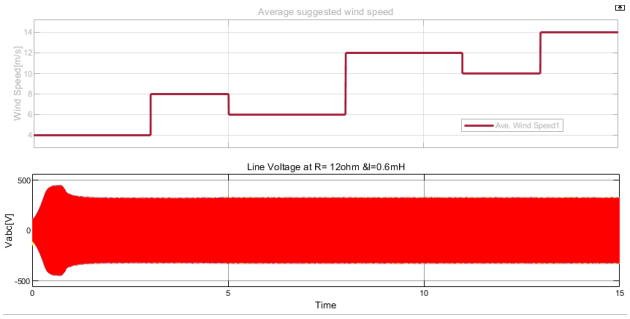

Figure 12. 3- Phase Voltage with variable wind speed.

The (THD) of the system for RL-load is shown in "Fig. 13", at start time 8s with 12 m/s is 1.46%. This figure describes the harmonics and distortions of the voltage and frequency waveform and determines their values.

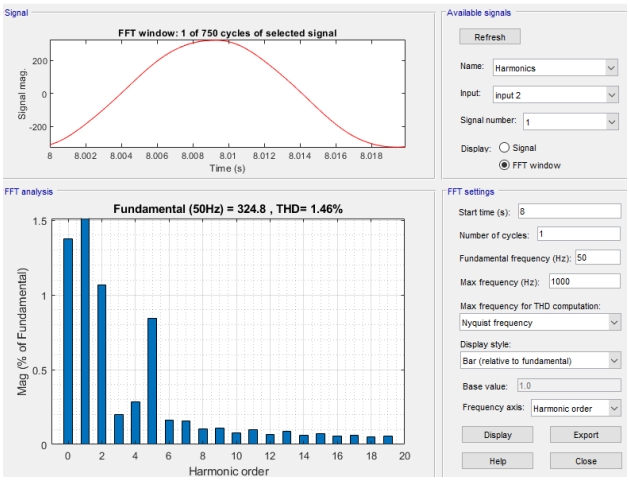

Figure 13. Total Harmonic Distortion in RL-Load

2. Conclusion

The SEIG model was presented using Matlab Simulink, where the FC-TCR control system was successfully used to ensure obtaining a three-phase sine voltage wave regardless of the change in wind speed and a constant frequency and work under pure resistance loads, resistance load, and inductance as the generated voltage follows the constant changes of wind speed. The excitation values of the capacitors connected across the generator's terminals were calculated to maintain the level of safety saturation within certain limits and avoid the high levels of saturation or its loss.

Acknowledgments

We want to thank the Electrical Engineering Department at the College of Engineering, University of Al-Mustansiriyah, for completing this research. We thank all colleagues who also helped us.

Conflict of interest

The publication of this article does not cause any conflict of interest with any other publication and is only for the Journal of Engineering and Sustainable Development (JEASD).

Abbreviations

IG	induction generator
SEIG	Self- excited induction generator
FC-TCR	Fixed capacitor-Thyristor control reactor
PI	Proportional integrations
VAR	Volt Ampere Reactive
DC	Direct Current
PWMSI	Pulse width modulation source inverter
AC	Alternating current
GA	genetic algorithm
MPPT	The maximum power point tracking
ITIBC	the instantaneous torque impulse balance control
S	Apparent power in VA
P	Active power in W
Q	Reactive power in VAR
THD	Total Harmonic distortion

3. References

1. Y. Chaturvedi, & A. Goel, (2019). "*Wind Powered Electricity Generation through Self Excited Induction Generator.*" World Scientific News, Vol.121, pp. 95-105.
2. B. Sawetsakulanond, & V. Kinnares, (2010). "*Design, analysis, and construction of a small scale self-excited induction*

generator for a wind energy application." Energy, Vol. 35, pp. 4975-4985.

3. N. Kabache, S. Moulahoum, & H. Houassine, (2014). "*Experimental investigation of self-excited induction generator for insulated wind turbine."* Journal of Electrical Engineering, Vol. 14, pp. 1-10.
4. J. Dalei, & K. B. Mohanty, (2015). "*Performance improvement of three-phase self-excited induction generator feeding induction motor load."* Turkish Journal of Electrical Engineering & Computer Sciences, Vol. 23, pp. 1660-1672.
5. K. S. Sakkoury, S. Emara, & M. K. Ahmed, (2017). "*Analysis of wind driven self-excited induction generator supplying isolated DC loads."* Journal of Electrical Systems and Information Technology, Vol. 4, pp. 257-268.
6. R. E. Raj, C. Kamalakannan, & R. Karthigaivel, (2017). "*Genetic algorithm-based analysis of wind-driven parallel operated self-excited induction generators supplying isolated loads."* IET Renewable Power Generation, Vol. 12, pp. 472-483.
7. T. Amieur, D. Taibi, & O. Amieur, (2018). "*Voltage oriented control of self-excited induction generator for wind energy system with MPPT."* In AIP Conference Proceedings (Vol. 1968, No. 1, p. 030067). AIP Publishing LLC.
8. Y. Wang, H. Gu, & W. Hao, (2019). "*An induction generator system based on instantaneous torque impulse balance control (ITIBC)."* IEEE Transactions on Power Electronics, Vol. 34, pp. 12296-12309
9. Y. Liu, M. A. Masadeh, & P. Pillay, (2020). *"Emulation of an Isolated Induction Generator under Unbalanced Conditions."* In 2020 IEEE Energy Conversion Congress and Exposition (ECCE) pp. 1794-1799. IEEE.
10. E. Touti, R. Pusca, J. F. Brudny, & A. Chaari, (2017). "*Self-excited Induction Generator in Remote Site."* In Reactive power control in AC Power Systems pp. 517-545. Springer, Cham.
11. D. Chermiti, & A. Khedher, (2014). "*Self-excited Induction Generator Using a Thyristor Controlled Reactor: frequency regulation and reactive Power Compensation*." In 2014 15th international conference on sciences and techniques of automatic control and computer engineering (STA) pp. 661-667. IEEE.
12. A. Hameed, A. Shaltout, & M. Abdel-Aziz, (2008). "*Frequency control of self-excited Induction Generator in Autonomous wind-Energy System."* In 2nd international conference on advanced control circuits and systems.
13. S. Kumar, & K. Gaur, (2013). "*Excitation process in three phase squirrel cage induction generator for windmill application."* In 2013 International Conference on Energy Efficient Technologies for Sustainability pp. 414-419. IEEE.
14. M. Stiebler, (2008). "*Wind energy systems for electric power generation."* Type of work (Book), Springer Science & Business Media, DOI: ISBN: 3540687653
15. S. Mathew, (2006). "*Wind energy: fundamentals, resource analysis and economics"* type of work (Book), Springer, DOI: ISBN: 3540309055
16. 16. T. Ramos, M. F. Medeiros Júnior, R. Pinheiro, & A. Medeiros, (2019). "*Slip Control of a Squirrel Cage Induction Generator Driven by an Electromagnetic Frequency Regulator to Achieve the Maximum Power Point Tracking"*. Energies, Vol. 12, pp. 2100.

17. S. Kannadhasan, M. Saravanapandi, C. Gurunathan (2018) "*Simulation and Analysis of Variable Speed Wind Turbine Coupled with Self-Excited Induction Generator*" International Journal of Trend in Scientific Research and Development (ijtsrd), ISSN: 2456-6470, Vol. 2 Issue-3, pp. 1622-1625, URL: https://www.ijtsrd.com/papers/ijtsrd11387.pdf
18. D. K. Mallik, & j. Ahmed, (2018). *Analysis of Self Excited Induction Generator for Standalone Micro-Hydro Scheme*. ADBU Journal of Electrical and Electronics Engineering (AJEEE), Vol. 2, pp. 22-31.
19. G. Ofualagba, & E. U. Ubeku, (2011*). "The analysis and modelling of a self-excited induction generator driven by a variable speed wind turbine"*. Fundamental and Advanced Topics in Wind Power, pp. 5-9.
20. S. Khandelwa, A. Agarwal, V. Agarwal, (2013) *"Matlab Based Analysis of 3-Ø Self-Excited Induction Generator with Nonlinear Load"* IOSR Journal of Electrical and Electronics Engineering, pp. 21-29